

PF127 aided preparation of super-porous TiO₂ film used in highly efficient quasi-solid-state dye-sensitized solar cell

Zhang Lan · Jihuai Wu · Jianming Lin ·
Miaoliang Huang

Received: 19 November 2009 / Accepted: 12 February 2010 / Published online: 24 February 2010
© Springer Science+Business Media, LLC 2010

Abstract The super-porous TiO₂ film is prepared with the block copolymer Pluronic F-127 as porous template. Comparing with the commonly used meso-porous TiO₂ film prepared with Polyethylene glycol 20,000 as pore former, the super-porous TiO₂ film shows higher photovoltaic performance when integrated it into polymer gel electrolyte based quasi-solid-state dye-sensitized solar cell (QS-DSSC). The enhanced dye adsorption, light scattering properties of the super-porous TiO₂ film improve the utilization efficiency of sun light to be converted to electricity. Moreover, the special microstructures of the super-porous TiO₂ film also makes for the deep penetration of polymer gel electrolyte into the dye-coated TiO₂ film, which is the prerequisite for highly photovoltaic performance of polymer gel electrolyte-based dye-sensitized solar cell. So it presents a feasible way to enhance the photovoltaic performance of QS-DSSC.

1 Introduction

The dye-sensitized solar cell (DSSC) reported by Grätzel in 1991 promised an easy, low-cost fabricating way to prepare solar cell comparing with the conventional photovoltaic

solar cell [1]. Recently, the energy conversion efficiency of DSSC has been achieved up to 11.18% [2]. However, the long-term performance of DSSC is poor due to the leakage, volatilization and other potential problems existing in liquid electrolytes, so higher stable solid or quasi-solid electrolytes are needed to substitute liquid electrolytes [3]. Both quasi-solid-state DSSC (QS-DSSC) and all-solid-state DSSC (AS-DSSC) now exhibit lower energy conversion efficiencies than that of liquid electrolyte based DSSC [4]. Therefore, further improvements of QS-DSSC or AS-DSSC are necessary. The key issues appear to be the improvements of the photovoltaic performance of dye-coated TiO₂ films.

Controlling the microstructures of TiO₂ film is particularly important since it is critical in governing the electronic properties of TiO₂ film. The conventional method for controlling the microstructures of TiO₂ film is through the addition of different amount of polyethylene glycol (PEG) 20,000 as pore former by burning it away [5]. A limitation of this method is that the fabrication of super-porous film needs large amount of PEG, which causes the poorer bonding strength among TiO₂ nanoparticles and the slower electronic transporting speed. A promising approach to fabricate super-porous film is based on the template of block copolymers. With the method, inorganic precursors are embedded in one domain of micro-phase separated by block copolymer. These hybrids can subsequently be transformed into a nano-structured/meso-porous ceramic by sintering the hybrids. It has been demonstrated that TiO₂ film prepared with block copolymer template can exhibit higher photovoltaic performance comparing with particle-based meso-porous film when integrated into the thin film liquid electrolyte based DSSC [6]. However, this approach is mainly through sol–gel route, which limits the thickness of the film and the crystallinity of TiO₂ nanoparticles for

Z. Lan (✉) · J. Wu (✉) · J. Lin · M. Huang
The Engineering Research Center of Environment-Friendly Functional Materials, Ministry of Education, Quanzhou, China
e-mail: lanzhang@hqu.edu.cn

J. Wu
e-mail: jhwu@hqu.edu.cn

Z. Lan · J. Wu · J. Lin · M. Huang
The Key Laboratory of Functional Materials for Fujian Higher Education, Institute of Materials Physical Chemistry, Huaqiao University, 362021 Quanzhou, China

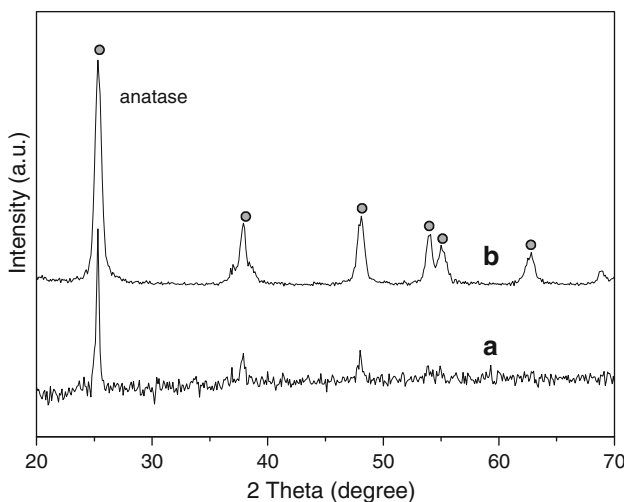


Fig. 1 X-ray diffraction patterns of TiO_2 powders after sintering at 450°C for 30 min, **a** with sol-gel method, **b** with hydrothermal method at 200°C for 12 h

further improving photovoltaic performance of DSSC. Clearly, effective operation of DSSC is achieved with the present state of art (i.e., the assembly of 10–20 nm sized well crystal TiO_2 nanoparticles).

Here, we report the fabrication of super-porous TiO_2 film, which maintains the present state of art, and introduces the super-porous morphology through the aid of

block copolymer Pluronic F-127 [poly(ethylene oxide)₁₀₆-poly(propylene oxide)₇₀-poly(ethylene oxide)₁₀₆] template. Comparing with the sol–gel route containing block copolymer template, the as prepared TiO_2 film contains higher crystal quality of TiO_2 nanoparticles and the thickness of the film can be extended to tens of micrometers without crack. When integrated it into highly conductive polymer gel electrolyte based QS-DSSC, an energy conversion efficiency of 7.93% was achieved.

2 Experimental

2.1 Materials

Tetra-*n*-butyl titanate, nitric acid, glacial acetic acid, polyethylene glycol 20,000, Pluronic F-127 [poly(ethylene oxide)₁₀₆-poly(propylene oxide)₇₀-poly(ethylene oxide)₁₀₆] are all A. R. grade and purchased from Sinopharm Chemical Reagent Co., Ltd, China. All reagents were used without further treatment.

Conducting glass plates (FTO glass, Fluorine doped tin oxide over-layer, sheet resistance $8 \Omega \square^{-1}$, purchased from Hartford Glass Co. USA) were used as substrates for precipitating TiO_2 porous film. Sensitizing dye *cis*-[$(\text{dcbH}_2)_2 \text{Ru}(\text{SCN})_2$] was purchased from Solaronix SA.

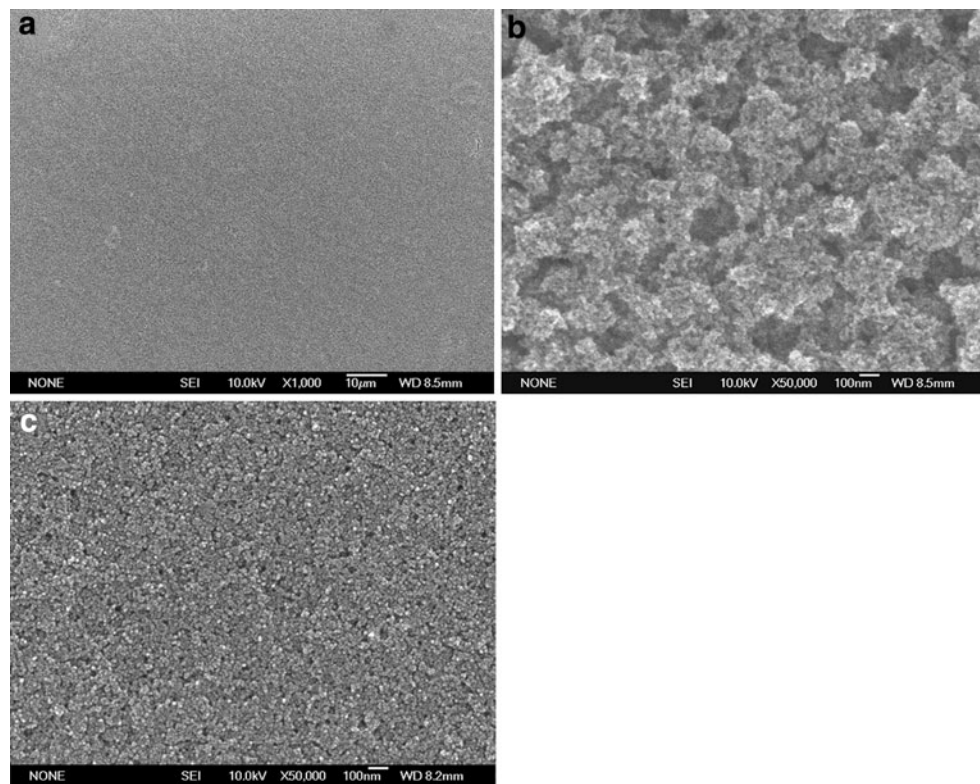


Fig. 2 SEM images of TiO_2 films fabricated with TiO_2 pastes containing PF127 (**a**, **b**) and PEG 20,000 (**c**)

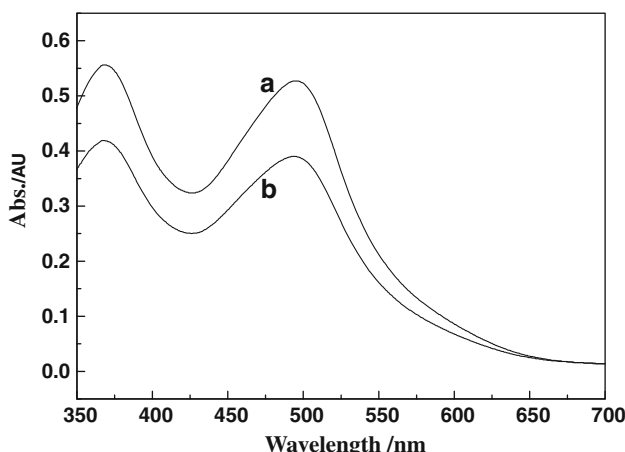


Fig. 3 UV–Vis absorption spectra of the dye-sensitized super-porous (a) and meso-porous (b) TiO₂ films

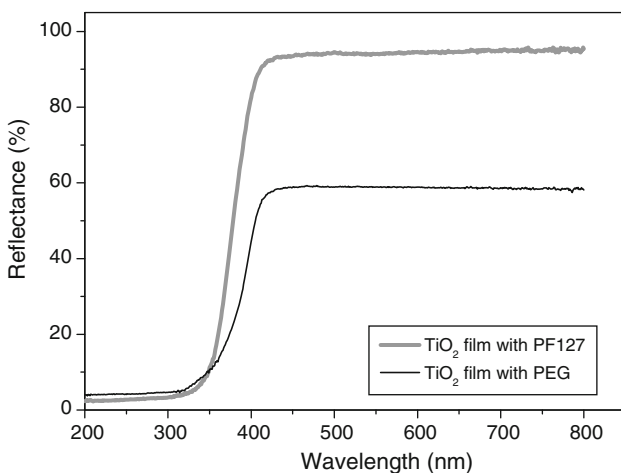


Fig. 4 UV–Vis diffuse reflectance spectra of the super-porous and meso-porous TiO₂ films (thickness of 18–20 μm)

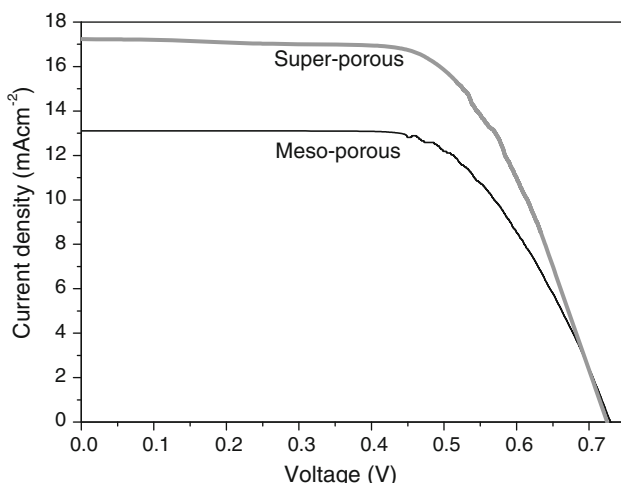


Fig. 5 I–V curves of polymer gel electrolyte based QS-DSSCs with super-porous/meso-porous TiO₂ films

2.2 Preparation of super-porous and meso-porous TiO₂ films

A thin TiO₂ blocking layer was firstly fabricated above the FTO glass [7], then the super-porous and meso-porous TiO₂ films were fabricated above it. The super-porous TiO₂ film is prepared as the following processes: the paste containing 10 g 10–20 nm TiO₂ nanoparticles, 1 g PF127, 2 mL propylene carbonate (PC) and 20 mL deionized water was firstly prepared, due to the hydrophobic property of polypropylene glycol (PPO) part in PF127, it could be selectively swollen by PC in the paste to form the porous template. Then the paste is precipitated on the FTO glass with a thin TiO₂ blocking layer with doctor blade method, the super-porous TiO₂ film was obtained after sintering the film at 450 °C for 30 min. For comparison, the meso-porous TiO₂ film was also prepared with the same methods as aforementioned, the different is that the 1 g PEG was substituted with 1 g PF127 in the latter paste. Then, the films were sensitized with 2.5×10^{-4} M absolute ethanol solution of *cis*-[(dcbH₂)₂Ru(SCN)₂] for 24 h. A new kind of highly conductive polymer gel electrolyte prepared by soaking poly (acrylic acid)-poly (ethylene glycol)-polypyrrole (PAA-PEG-PPy) hybrid in 30 vol.% *N*-methyl pyrrolidine (NMP) and 70 vol.% γ -butyrolactone (GBL) mixed solvents with 1.0 M NaI, 0.15 M I₂ and 0.4 M pyridine was used for QS-DSSC. The ionic conductivity of the polymer gel electrolyte is 8.156 mS cm⁻¹, equivalent with that of liquid electrolyte. More details about fabrication of 10–20 nm TiO₂ nanoparticles, polymer gel electrolyte and QS-DSSC are all the same as our previous papers [8, 9].

2.3 Measurements

The morphologies of super-porous and meso-porous TiO₂ films were analyzed by SEM. The crystallization of nanocrystalline TiO₂ particles was measured by X-ray diffractometer using Cu K α radiation (λ) 1.5405 Å. The diffuse reflectance and dye-adsorption spectra of TiO₂ films were measured with UV–visible spectrophotometer. The adsorbed dyes were washed from dye-coated TiO₂ films with 0.1 M NaOH ethanol solution before measurement. The photovoltaic tests of QS-DSSCs were carried out by measuring the I–V characteristic curves under simulated AM 1.5 solar illumination at 100 mW cm⁻², from a xenon arc lamp (CHF-XM500, Trusttech Co., Ltd, China) in ambient atmosphere and recorded with CHI 660 C electrochemical workstation. The thickness of photo electrode and the active area of QS-DSSC were 18–20 μm and 0.5 cm² (1 × 0.5 cm²), respectively.

Table 1 The parameters of the QS-DSSCs with different morphologies of TiO₂ films

TiO ₂ film	BET surface area (m ² g ⁻¹)	Porosity (%)	Adsorbed dye (10 ⁻⁵ mol cm ⁻²)	V _{OC} (V)	J _{SC} (mA cm ⁻²)	FF	η (%)
Super-porous	56	63	4.85	0.725	17.24	0.635	7.933
Meso-porous	41	45	3.64	0.729	13.11	0.646	6.172

3 Results and discussion

Figure 1 shows the X-ray diffraction patterns of TiO₂ powders after sintering at 450 °C for 30 min. The standard 2θ characteristic peaks of anatase TiO₂ according to the JCPDS#21-1272 are at 25.3°, 37.55°, 47.85°, 53.75°, 55.05° and 62.35°, which are all existed in the X-ray diffraction patterns of TiO₂ powders prepared with both hydrothermal and sol-gel methods, so it is verified that the crystallization of TiO₂ powders is anatase. The characteristic peaks of anatase in X-ray diffraction patterns of TiO₂ powders prepared with hydrothermal method is clearer and stronger than that of TiO₂ powders prepared with sol-gel method, so the former TiO₂ powders show higher crystallinity, better crystal perfection, lower strain, and larger crystal sizes than that of the latter one. It is known that the highly photovoltaic performance of DSSC can be obtained with highly crystal quality of TiO₂ nanoparticles, so it can be expected that the photovoltaic performance of DSSC with super-porous TiO₂ film by the present state of art will be better than that of the DSSC with TiO₂ film by the sol-gel method [10].

Figure 2 shows the SEM images of TiO₂ films fabricated with TiO₂ pastes containing PF127 (a, b) and PEG 20,000 (c). It is seen from Fig. 2 that the TiO₂ film prepared with PF127 is homogeneous at the micro-scale without cracks, and there are many sub-micro size holes uniformly dispersing in the film, so it is named as super-porous TiO₂ film. The TiO₂ film prepared with PEG 20,000 (Fig. 2c) shows meso-porous microstructure. The diameter of the holes is much smaller than that of the super-porous TiO₂ film.

The UV-vis absorption spectra of the dye-coated super-porous and meso-porous TiO₂ films are shown in Fig. 3. It is seen that the amount of adsorbed dye by the super-porous TiO₂ film is larger than that of the meso-porous TiO₂ film. The different morphologies of the two kinds of films answer for the above results. For the super-porous TiO₂ film, apart from the sub-micro size holes existing in the film, there still exists many nano-size holes among the network of the film, so it is just like a sponge, the dye solution can easily penetrate into the film and soak most of TiO₂ nanoparticles [11]. Moreover, the higher BET surface area as listed in Table 1 is also benefit for dye loading on the film. While for the meso-porous TiO₂ film, the holes

are small and do not uniformly disperse in the film, some TiO₂ nanoparticles are bonded too compactly to form holes, which are not benefit for the penetration and soaking of dye solution, so the amount of adsorbed dye in the meso-porous TiO₂ film is less than that of the super-porous TiO₂ film.

It is verified that voids embedded in the TiO₂ film can be used as light scattering center [12]. The scattering characteristics of the super-porous and meso-porous TiO₂ films are investigated with UV-vis diffuse reflecting spectra as shown in Fig. 4. The reflecting rate of the super-porous TiO₂ film is stronger than that of the meso-porous TiO₂ film. Optical simulations indicated that the diameter of voids for efficient scattering center should be larger than 100 nm [13], the holes in the super-porous TiO₂ film meet the prerequisites, so it shows highly reflecting efficiency.

I-V curves of QS-DSSCs are presented in Fig. 5. The relative parameters of the QS-DSSCs with super-porous and meso-porous TiO₂ films are listed in Table 1. It is seen that the QS-DSSC with super-porous TiO₂ film shows higher photovoltaic performance than that of the QS-DSSC with meso-porous TiO₂ film. The larger amount of adsorbed dye and higher reflecting efficiency of super-porous TiO₂ film result in higher short-circuit current density [14]. Moreover, the larger porosity of super-porous TiO₂ film is also benefit for the deep penetration of polymer gel electrolyte, which also enhances the photovoltaic performance of the QS-DSSC.

4 Conclusions

In conclusion, the super-porous TiO₂ film is prepared with the aid of the block copolymer Pluronic F-127 and 10–20 nm TiO₂ nanoparticles. It shows larger amount of adsorbed dye and higher reflecting efficiency than that of the meso-porous TiO₂ film. When combined it with highly conductive polymer gel electrolyte based QS-DSSC, energy conversion efficiency about 7.93% is achieved. So it presents a feasible way to fabricate highly photovoltaic performance of QS-DSSC.

Acknowledgments The authors would like to acknowledge the support of the National High Technology Research and Development

Program of China (No. 2009AA03Z217), the National Natural Science Foundation of China (No. 50572030, 50842027), and the Natural Science Foundation of Hua Qiao University (No. 09BS401).

References

1. B. O'Regan, M. Grätzel, *Nature* **353**, 737 (1991)
2. M.K. Nazeeruddin, F. De Angelis, S. Fantacci, A. Selloni, G. Viscardi, P. Liska, S. Ito, B. Takeru, M. Grätzel, *J. Am. Chem. Soc.* **127**, 16835 (2005)
3. J. Kruger, R. Plass, M. Grätzel, H.J. Matthieu, *Appl. Phys. Lett.* **81**, 367 (2002)
4. P. Wang, S.M. Zakeeruddin, J.E. Moser, M.K. Nazeeruddin, T. Sekiguchi, M. Grätzel, *Nat. Mater.* **2**, 498 (2003)
5. C.J. Barbe, F. Arendse, P. Comte, M. Grätzel, *J. Am. Ceram. Soc.* **80**, 3157 (1997)
6. M. Zukalova, A. Zukal, L. Kavan, M.K. Nazeeruddin, P. Liska, M. Grätzel, *Nano Lett.* **5**, 1789 (2005)
7. J.H. Wu, S.C. Hao, Z. Lan, J.M. Lin, M.L. Huang, Y.F. Huang, P.J. Li, T. Sato, *J. Am. Chem. Soc.* **130**, 11568 (2008)
8. Z. Lan, J.H. Wu, S.C. Hao, J.M. Lin, M.L. Huang, Y.F. Huang, *Energy Environ. Sci.* **2**, 524 (2009)
9. J.H. Wu, Z. Lan, J.M. Lin, M.L. Huang, S. Yin, T. Sato, *Adv. Mater.* **19**, 4006 (2007)
10. M. Grätzel, *Inorg. Chem.* **44**, 6841 (2005)
11. M.J. Cass, F.L. Qiu, A.B. Walker, A.C. Fisger, L.M. Peter, *J. Phys. Chem. B* **107**, 113 (2003)
12. S. Hore, P. Nitz, C. Vetter, C. Prahl, M. Niggemann, R. Kern, *Chem. Commun.* 2011 (2005)
13. J. Ferber, J. Luther, *Sol. Energy Mater. Sol. Cells* **54**, 265 (1998)
14. S. Nakade, M. Matsuda, S. Kambe, Y. Saito, T. Kitamura, *J. Phys. Chem. B* **105**, 12433 (2001)